Methane production by CO 2 hydrogenation reaction with and without solid phase catalysis

Stefano Falcinelli, Andrea Capriccioli, Fernando Pirani, Franco Vecchiocattivi, Carles Martí Aliod, Andrea Nicoziani, Emanuele Topini, Antonio Lagana

Methane production by CO_2hydrogenation reaction with and without solid phase catalysis

Stefano Falcinelli[a,], Andrea Capriccioli[b], Fernando Pirani[c], Franco Vecchiocattivi[a], Stefano Stranges[d], Carles Martì[c], Andrea Nicoziani[c],Emanuele Topini[a], and Antonio Laganà[e]*

[a]*Department of Civil and Environmental Engineering, University of Perugia, Via G. Duranti 93, 06125 Perugia, Italy.*

[b]*ENEAC.R. Frascati, Via E. Fermi 45, 00044 Frascati, Italy.*

[c]*Department of Chemistry, Biology and Biotechnologies, University of Perugia, Via Elce di Sotto 8, 06123 Perugia, Italy.*

[d]*Department of Chemistry and Drug Technology, University of Rome "La Sapienza", 00185 Rome, Italy.*

[e]*Master-up srl, Via Elce di Sotto 8, 06123 Perugia, Italy*

[*] Corresponding author: Tel. +39 0755853856, - 5527; Fax: +39 0755853864; E-mail: stefano.falcinelli@unipg.it (S. Falcinelli).

https://doi.org/10.1016/j.fuel.2017.07.109

Abstract

Leveraging on the experience gained by designing and assembling a prototype experimental apparatus reusing $CO_2$to produce methane in a reaction with H_2, we are developing an alternative innovative cost effective and contaminant resistant synthetic strategy based on the replacement of the solid phase catalysiswith a homogeneous gas phase processgoing through the forming CO_2^{2+} molecular dications.

Keywords: methanation reactor;CO_2 waste;free methane; catalyst; plasma, dications.

Introduction

As reported during the 2nd SMARTCATs general meeting of the COST Action CM1404 we are carrying out a research aiming at re-using CO_2 and implementing a *validated laboratory technology* based on an experimental prototype apparatus (called ProGeo) producing carbon neutral methane through the chemical conversion of CO_2 waste flue gases using renewable energies.

The research is being carried out in collaboration by researchers of the laboratories of the University of Perugia and of ENEA (the Italian National Agency for New Technologies, Energy and Sustainable Economic Development of Frascati) with the support of a cluster of Small and Medium-sized Enterprises (SME)s coordinated by the Master-up srl company.In particular, the project leverages a) on the expertise of the Departments of Chemistry, Biology and Biotechnology and of Civil and Environmental Engineering of the University of Perugia on the experimental and theoretical treatment of elementary reactive and non reactive molecular processes [1-8] and b) on the engineering capabilities of designing, building and experimenting innovative apparatuses of ENEA [9] researchers with the support of the above mentioned SMEs specialized in the field of molecular science software modeling.Such

49 collaboration has been incubated by the networking activities of some COST actions [10,11]
50 and of some virtual communities of the European Grid Infrastructure EGI.eu [12, 13].
51 The first purpose of this paper is to illustrate how the developed distributed computing
52 machinery (i.e. the collaborative (workflowed) sharing of high level accurate and approximate
53 ab initio and empirical calculations of the electronic structure of the involved molecular
54 systems, the fitting and, as an alternative, force field formulations of the related potential
55 energy surfaces together with accurate quantum, quantum-classical, quasi-classical
56 dynamicalcalculations of the detailed properties of the system plus their integration with
57 statistical averaging of the detailed properties over the unobserved parameters as well as their
58 combination in multi-scale treatments) has provided a solid ground for a converging
59 comparison of experimental and computational investigationsof the methane formation from
60 CO_2usingsolid state catalyzed processes.
61 The second purpose of the paper is to illustrate how the progress made in the above
62 mentioned research line has prompted a new one based on the use of the Synchrotron and the
63 Free Electron Laser light sources to investigate the possibility of developing routes alternative
64 to solid state catalyzed techniques. In particular, details are given on how CO_2 hydrogenation
65 can occur via plasma generation by either electrical discharges or by vacuum ultraviolet
66 (VUV) excitations of a $CO_2 + H_2$ gas mixture.
67 Accordingly, the paper is articulated as follows:
68 in section 2 structure and performances of the methanation reactor are illustrated;
69 in section 3 the computer simulation of the involved processes is analysed;
70 in section 4 the research lines driving the evolution of the apparatus towards a pure gas phase
71 one are discussed.
72
73

2. The present methanation reactor

Experimental measurements of methane yields of *ProGeo* have been carried out using CO_2 bottles (some measurements have been performed alsousing CO_2 produced (in the ratio of 1.9 kg per litre) from grapes fermentation of Marsala, a famous wine of the region where Garibaldi got ashore when starting the unification of Italy, kindly provided by IRVO (Istituto Regionale Vini e Oli)). The measurements show a complete compatibility with the catalyser used for the methanation process in *ProGeo*. The used catalyser is $KATALCO_{JM}$ 11-4MR a commercial product of the Johnson Matthey company (made of silicate hydrous aluminum, silicon oxide, nickel, nickel oxide, magnesium oxide, graphite porous small cylinders of average diameter 3.1 mm and height 3.6 mm containing metallic nickel) whose 2500X micrography is shown in Fig. 1.

The ProGeo reactor is designed for an exit CH_4 maximum flux of 1 Nm^3/h. As shown in Figure 2, it is articulated in twin columns (twin flow channels) externally cooled thanks to shared laminar elements in order to dissipate the heat produced by the exothermicity of the reaction (ΔH_{298K}=-164.9 kJ mol^{-1}). Design parameters of the reactor are:

GHSV (Gas Hourly Space Velocity) (ml h^{-1} gr^{-1}) and SV (Space Velocity) (h^{-1}).

Another useful parameter is the ratio between the total flux of gas and the exposed surface of the catalyser indicated as GHCS (Gas Hourly Catalyst Surface) (cm h^{-1}).

The value of the reactor parameters of the present version of the ProGeo apparatus are: GHSV = 3200 ml $h^{-1}gr^{-1}$ and SV = 2100 h^{-1} leading to a GHCS parameter of 155 cm h^{-1}.

The resulting features of the present ProGeo apparatus shown in Fig. 2 are:

- External diameter of the single channel 60 mm;
- Catalysed total length 660 mm;
- Maximum inlet flux (H_2+CO_2) 6 Nm^3/h;

- Reference Molar ratio (CO_2/H_2) 1/5;
- Maximum outlet flux (CH_4) 1 Nm^3/h.

Experimental measurements have been carried out by varying:

- the CO_2/H_2 molar ratio from a minimum of 1/4 to a maximum of 1/5.5;
- the reactor temperature from a minimum of 220 °C to a maximum of 450 °C;
- the H_2 flux from a minimum of 0.8 Nm^3/h to a un maximum of 2.5 Nm^3/h;
- the pressure from a minimum of 1 bar to a maximum of 2 bar.

A key element for a quantitative measurement of the reaction yield is the regular monitoring of the temperature both along the central axis of each channel (maximum temperature) and along the peripheral axis (minimum temperature). In Figure 3 the location and labels of the channel thermocouples (6 axial and 3 peripheral) are shown as dots together with the cross section of the twin columns.

The methanation reactions occur mainly on the top segment of the reactor close to the inlet (90% in the first 200 mm). Accordingly, most of the produced heat is detected by the central thermocouples (T5, T6 and T14, T15). The average of the measured percentage of produced methane is plotted as a function of the molar ratio and temperature in Fig. 4. As is apparent from the Figure, the threshold temperature is 240°C and the range of temperature of optimal yield is 300 - 350°C. The molar ratio has a significant impact on the percentage of produced methane with the optimum value of the CO_2 / H_2 ratio being 1/5.

3. Computational simulation of methane production from the CO_2+H_2 reaction with solid phase catalysis

In our laboratory the initial rationalization of the processes involved in producing methane via the Sabatier reaction (i.e. by making H_2+CO_2 react on a catalytic surface [14]) has been

performed by following the flowchart of ZACROS [15], a Kinetic Monte Carlo (KMC) [16,17] software package written in Fortran 2003. ZACROS leverages on the Graph-Theoretical KMC methodology coupled with both cluster expansion Hamiltonians for the ad-layer energetics and the Brønsted-Evans-Polanyi relations for the activation energies of elementary events [16]. ZACROS enables researchers in the areas of Computational Catalysis and Surface Science to perform dynamic modelling of adsorption, desorption, surface diffusion, and reaction processes on heterogeneous catalysts. Although in our traditional GEMS (Grid Empowered Molecular Simulator) [18] approach based on distributed computing platforms the rates (r) of elementary processes are computed by running molecular dynamics calculations based on Potential Energy Surfaces (PES)s originating from *ab initio* treatments, in the version of ZACROS implemented by us, for all the elementary steps potentially participating in the mechanism, the values of r to be used are taken from the literature and are usually given the following Transition State (TS) theory formulation [19,20]

$$r = A \cdot \exp\left(-\frac{E_a}{k_B T}\right) \quad (1)$$

in which A is a pre-exponential factor (quantifying the propensity of the system to cross from TS to products) while the exponential term brings in the information on the PES of the related elementary process (either forward "f" or backward "b") as the energy difference E_a between the stationary point of the potential Minimum Energy Path (MEP) at the transition state and that associated with the reactant asymptote with k_B being the usual Boltzmann constant and T the temperature. The lowest approximation level formulates the pre-exponential factor as $k_B T/h$ where h is the Plank constant.

In the adsorption of gaseous species, however, the most frequently used expression for the rate of reaction is the well known Hertz-Knudsen equation:

$$r_i^{ad} = S_{0,i} \cdot A_{site} \frac{p_i}{\sqrt{2\pi m_i k_B T}} \quad (2)$$

where $S_{0,i}$ is the sticking coefficient (for which we take the value 1 in this work),A_{site} is the area of the adsorption site, p_i is the partial pressure of species i and m_i its mass.

A more accurate formulation of the rate coefficients makes use of the partition function for both, the intermediate state (incorporating so far the information about the remaining degrees of freedom) and the reactants:

$$A = \left(\frac{k_B T}{h}\right)\left(\frac{Q^{\neq}}{Q_r}\right) \quad (3)$$

where $Q^{\neq}$ is the transition state partition function and Q_r the partition function of reactant species.

Each partition function is calculated considering that rotations and translations are frustrated (hindered), due to the fact that they are adsorbed, and therefore can be assimilated to vibrational degrees of freedom. In that case, the vibrational partition function takes the form:

$$Q_{vib,X} = \prod_k \frac{\exp\left(\frac{-h\nu_k}{2k_B T}\right)}{1-\exp\left(\frac{-h\nu_k}{k_B T}\right)} \quad (4)$$

where $Q_{vib,X}$ is the total vibrational partition function of the species$X$, and ν_k is the frequency of the vibrational mode k.

In this way ZACROS can also simulate desorption/reaction spectra at a given temperature providing so far a rationale for designing kinetic mechanisms and understanding experimental data.

163 The elementary processes considered for the simulations are given in refs. [21,22] together
164 with the numerical value of the related parameters. Hexagonal periodic default lattice will be
165 the one of our choice for the Ziff, Gulari and Barshad (ZGB) reference model [23] as well as
166 for the Sabatier Process.

167 An important outcome of our calculations is illustrated in Fig. 5 (see also ref. [19]) in which,
168 in contrast with the suggestion of ref. [21] of a dominance of the CO* decomposition, it is
169 apparent from the analysis of the ZACROS calculations that the dominant process leading to
170 the production of CH_4 is the hydrogenation of CO. This has suggested us to investigate
171 possible alternative gas phase processes producing CO. For this reason, we decided to
172 investigate the possibility of inducing CO_2 dissociation and producing CO+O and CO^++O^+
173 neutral and ionic chemical pairs reacting with hydrogen, respectively, via a plasma generation
174 either by electrical discharges or by vacuum ultraviolet (VUV) photons on a CO_2+H_2 gas
175 mixture as will be discussed in the next section.
176

177 **4. Methane production from the CO_2+H_2reaction without solid phase catalysis**

178 The investigations carried out on our ProGeo 20kW apparatus [22] based on the well
179 known Sabatier reaction:

180 $$CO_2 + 4\ H_2 \leftrightarrows CH_4 + 2\ H_2O \qquad \Delta H^{\circ}_{298} = -165\ \text{kJ mol}^{-1} \qquad (5)$$

181 at moderately high pressure (2-3 atm) and high temperature (200-300°C) with the use of a
182 solid phase catalyst (nickel, ruthenium, or alumina) has prompted us to further progress (as
183 will be illustrated in detail in this section) to use either low cost or renewable energy to reuse
184 waste CO_2 to produce methane in a circular economy scheme [22]. To this end we have
185 undertaken the investigation of a new methanation pathway aimed at avoiding the use of the
186 solid phase catalysis, by exploring mechanisms involving a plasma generation by electrical
187 discharges or by vacuum ultraviolet (VUV) photons on a CO_2+H_2 gas mixture.This effort is

188 based on the since long established expertise of our laboratories in promotingand modeling
189 molecular processes (atomic hydrogen and excited metastable species generation by electrical
190 discharge [24-26] to study gas phase processes induced under controlled conditions) and in
191 fully characterizing the microscopic dynamics of elementary reactions by experimentally
192 determining related main kinetic parameters such as rate constants, cross sections,
193 intermolecular potentials, structure, and energy of the transition state, reaction pathways,
194 etc.Furthermore, we can perform high resolution experiments in single collision conditions
195 using crossed molecular beam apparatuses and studying plasma induced gas phase reactions
196 both by microwave and RF (Radio Frequency) discharges [24-26] and by synchrotron
197 radiation [27-29]. In particular the mentioned experiments are performed on the crossed
198 molecular beams apparatus of the Perugia University [30,31] to measure PIES (Penning
199 Ionization Electron Spectroscopy) data, and on the ARPES (Angle Resolved PhotoEmission
200 Spectroscopy) end station at the GasPhase Beamline of the Elettra Synchrotron Radiation
201 Facility (Trieste) [32,33] (more details are given later in the specific subsection).
202 The need of avoiding the use of the solid phase catalyst to perform reaction (5) and
203 investigating possible alternative microscopic reaction mechanisms occurring in the
204 homogeneous gas phase, is motivated by concurrency of reaction (5) and the following two
205 main reactions:

206 $$CO + 3\ H_2 \leftrightarrows CH_4 + H_2O \qquad \Delta H^\circ_{298} = -206{,}1\ kJ\ mol^{-1} \qquad (6)$$

207 $$CO + H_2O \leftrightarrows H_2 + CO_2 \qquad \Delta H^\circ_{298} = +41\ kJ\ mol^{-1} \qquad (7)$$

208 as well as by the wish of avoiding unwanted reactions, like the (8), (9), (10), and (11) listed
209 below,

210 $$CO_2 + 2\ H_2 \leftrightarrows C + 2\ H_2O \qquad \Delta H^\circ_{298} = -90{,}1\ kJ\ mol^{-1} \qquad (8)$$

211 $$2\ CO \leftrightarrows C + CO_2 \qquad \Delta H^\circ_{298} = -172{,}4\ kJ\ mol^{-1} \qquad (9)$$

212 $$CO + H_2 \leftrightarrows C + H_2O \qquad \Delta H^\circ_{298} = -131{,}3\ kJ\ mol^{-1} \qquad (10)$$

$$CH_4 \leftrightarrows C + 2\,H_2 \qquad \Delta H^{\circ}_{298} = +74{,}8\ \text{kJ mol}^{-1} \qquad (11)$$

responsible for a rapid loss of catalytic activity. Further reservations on the use of a Ni based solid phase catalyst are related to the environmental and safety issues associated with the possible formation of $Ni(CO)_4$ that is a highly toxic gaseous species produced when Ni is exposed to a gas mixture containing high pressure CO as typical of experimental conditions commonly used to maximize the yield of CH_4 in the methanation reaction.

For this purpose we have undertaken the study of the Sabatier reaction (5) in a homogeneous gas phase environment by generating and characterizing controlled plasmas via electrical discharges and VUV photons on a pure CO_2 and CO_2+H_2 gaseous mixture a technology in which our research group is leader since early 1990 [24,34,35]. In our experimental apparatuses (described in the next section) the energy pumped in the produced plasma can be controlled using both electrons and photons. In the first case we use an inhouse electrical microwave or RF discharge. In the second case we use a tunable synchrotron radiation. At the same time we can control and characterize the chemistry of the generated plasmas by studying the microscopic dynamics of the elementary chemical reactions because in molecular beam techniques [38-40] they occur in single collision regime (see again below in the specific subsection).

4.1. Experimental methods

As already mentioned, a first attempt to produce plasmas containing carbon dioxide, has been made in our laboratory using a microwave discharge beam source operating in pure CO_2 and in an approximately 50-50% CO_2-H_2 mixture at a global pressure of about 1600 Pa. The microwave discharge is produced in a cylindrical quartz tube (10 cm in length and 2 cm in diameter) in a brass resonance cavity (water cooled) working at 2450 MHz [24,34,35]. The applied microwave power was varied in the range 70-200 W with a reflected power lower

than 5%. A preliminary characterization of the produced plasma has been performed using the crossed molecular beam apparatus shown in Figure 6. Such an apparatus, usually devoted to the study of the microscopic dynamics of autoionization reactions induced by excited metastable species (also called Penning Ionization or Chemi-ionization reactions), for the experiment considered here was used by keeping the secondary beam switched off. In this way it was possible to detect only the main chemical species flowing out of the plasma microwave discharge source as an effusive molecular beam. Such an analysis was performed using the mass spectrometry characterization of the beam by means of a quadrupole mass filter located below the crossing beams region. Measured data is consistent with that previously recorded by Dobrea *et al.* [39,40] who found a large dissociation rate of carbon dioxide, according to reactions (12) and (13) below, in the case of the plasma discharge in pure CO_2 with respect to the one measured in CO_2+H_2 gas mixture.

$$CO_2 + e^- \rightarrow CO + O \quad (12)$$

$$O + O \rightarrow O_2 \quad (13)$$

The CO_2 dissociation percentage, χ (determined by keeping the inlet gas pressure at a constant value of 1600 Pa) was obtained by recording the CO_2^+ intensities I_i and I_f (measured with the microwave discharge off and on, respectively) using the following relationship:

$$\chi = \frac{I_i - I_f}{I_i} \cdot 100 \quad (14)$$

The values of χ amounted to about 27% in the case of the plasma discharge in pure CO_2, and lowered to about 19% in the case of CO_2+H_2 gas mixture at an applied microwave power of 100 W. The measured values increased up to 52% (for plasma in pure CO_2) and 36% (in plasma in CO_2+H_2 mixture) when the microwave power was doubled to about 200 W. Measured data is reported in Table 1 and compared with that of refs. [39,40].

Then the same apparatus of Figure 6 was used to measure plasma-assisted CO_2 conversion into hydrocarbons as an alternative way of producing synthetic fuel (this technique has been

recently applied by Welzel *et al.* [41] who determined the experimental conditions suited to give a 20% yield for CH_4 formation. We better characterized the chemistry of the produced plasmas by investigating the detail of the chemical reactions induced by the ionic species that can be formed in such gaseous environments using VUV photons as a source of energy to induce excitation and ionization processes responsible for the plasma generation. The experiment was performed at the ELETTRA Synchrotron Light Laboratory (Trieste, Italy), using the ARPES end station at the Gas Phase having a very high photon intensity and a tunable wavelength. Details of the beam-line and of the end station have been already reported elsewhere [42,43] and the characteristics of the apparatus used for the experiment are discussed in detail in refs. [44,45]. Specific features of the experiment reported here are: i) the use of a synchrotron radiation tunable energy source, working in the energy range of 35-50 eV with a resolution of about 1.5 meV; ii) the detection of all produced charged particles (electrons and ions) in the generated plasma, recording them in a time resolved measurements in which we are able to extract the spatial momentum components of final ions by using the electron-ion-ion coincidence technique coupled with an ion position sensitive detector (see below).

Figure 7 shows: i) on the left hand side panel, a scheme of the main part of the experimental apparatus based on the electron-ion-ion coincidence technique, and, as an example, the coincidence plot recorded in the double photoionization experiment of carbon dioxide at a photon energy of 44 eV (in such a panel are also shown the recorded mass spectra of the product ions at the same photon energy); ii) on the right hand side panel, a picture of such a device. As can be seen from the Figure, the monochromatic synchrotron light beam crosses at right angles an effusive molecular beam of CO_2 neutral precursors, and the product ions are then detected in coincidence with photoelectrons. The coincidence electron-ion-ion extraction and detection system consists in a time of flight (TOF) mass spectrometer equipped with an

ion position sensitive detector (stack of three micro-channel-plates with a multi-anode array arranged in 32 rows and 32 columns). As mentioned above, such a detector has been especially designed in order to properly measure the spatial momentum components of the ionic products [46].

Carbon dioxide was supplied from a commercial cylinder at room temperature (99.99% nominal purity) to a needle effusive beam source. An adjustable leak valve along the input gas pipe line was used in order to control the gas flow, which was monitored by checking the pressure in the main vacuum chamber.

4.2. The chemical role of CO_2 in the generated plasma

When using excitation energies higher than 35 eV, it is possible to induce ionization phenomena in gaseous mixtures containing carbon dioxide with the production of CO^+, O^+ and CO_2^{2+} ions (as a matter of fact plasmas constitute over 99% of the known matter of the Universe). Indeed, the formation of doubly charged positive ions in gas phase using VUV photons or energetic electrons as ionizing source is routine in a number of laboratory experiments able to reproduce the physical conditions of the upper atmosphere of some planets of the Solar System (such as Mars, Venus, and Titan) [27-29, 49-52]. Once these ionic species are produced in metastable states, after their typical lifetime they can, dissociate into ionic fragments having a high kinetic energy content due to the strong Coulomb repulsion characterizing the low stability of their electronic structure. This so called "Coulomb explosion" of molecular dications provides their fragments with a large amount of translation energy (several eV) that enhances the chemical reactivity of the plasma with the following consequences on the properties of a gas mixtures: i) the chemical behavior is radically changed because the removed electrons may change sensibly the electronic configuration of the neutral species and modify its chemical reactivity; ii) the interaction is much more intense

than the neutral-neutral one, making more likely collision events and increasing the chemical reactivity in plasma environments; iii), the formation of fragment ions with large kinetic energy increase chemical reactivity.

In particular our experiments with a plasma containing CO_2 confirmed the carbon dioxide dissociation paths singled out by previous studies [53-56] and quantified the following ones allowed to indicates that the following main processes are possible with their respective threshold energies:

$$CO_2 + h\nu \rightarrow (CO_2^+)^* + e^- \rightarrow CO^+ + O^* + e^- \rightarrow CO^+ + O^+ + 2e^- \qquad h\nu \geq 35.6 \text{ eV} \qquad (15)$$

$$\rightarrow CO_2^{2+} + 2e^- \qquad h\nu \geq 37.3 \text{ eV} \qquad (16)$$

$$\rightarrow (CO_2^{2+})^*_{\text{long lived}} + 2e^- \rightarrow CO^+ + O^+ + 2e^- \qquad h\nu \geq 38.7 \text{ eV} \qquad (17)$$

together with relative threshold energies. In particular, reaction (15) is an indirect process occurring below the double photoionization threshold of 37.34 eV, via the formation an excited state of the $(CO_2^+)^*$ monocation, followed by the production of an intermediate autoionizing oxygen atom O^*. Reaction (16) produces a stable CO_2^{2+} dication. Reaction (17) mainly occurs via the formation of a long lived dication with lifetime $\tau \geq 3.1$ μs, corresponding to the production of CO_2^{2+} ions in the ground $X^3\Sigma^+_g$ electronic state with an internal energy below the threshold towards the Coulomb explosion [53-56].

Figure 8 shows the relative cross sections measured in the investigated photon energy range for reactions (15), (16), and (17) recorded using the electron-ion-ion coincidence technique discussed in the previous section. The analysis of data, collected at each investigated photon energy, is based on the density distribution evaluation of coincidences in the measured coincidence spectra, such as the one reported in the left panel of Fig. 7. On such an analysis, the total counts (recorded at each investigated photon energy) corresponding to the ion pair peak coming out from the same reaction gives the relative cross section for the three investigated reaction channels of Fig. 8. At the same time, the KER (Kinetic Energy

Released) of product ions can be evaluated by analyzing the dimension and the shape of the recorded peaks using the method suggested by Lundqvist *et al.* [57]. This procedure, applied to the CO^+/O^+ coincidences signal related to reactions (15), (16) and (17), has allowed us to evaluate the KER distributions of all product ions for different values of the investigated photon energy (36.0, 39.0, 41.0, 44.0 and 49.0 eV). The results shown in Fig. 9 tell us that the KER value for the O^+ ions ranges between 1.0 and 5.0 eV, while the CO^+ KER can reach 3.0 eV or more and, changes the maximum value depending on the investigated photon energies. These results demonstrate that the chemical reactivity of plasmas containing CO_2 is strongly increased by the presence of CO^+ and O^+ ions having a very high kinetic energy. In particular, the fast CO^+ ions, are expected to react with molecular and atomic hydrogen (both produced in a plasma generated by a microwave discharge in a gaseous CO_2+H_2 mixture [24-26, 39,40]) playing a pivotal role in the plasma-assisted CO_2 conversion on CH_4 fuel. In this respect, it has to be noted that Knott *et al.* measured reactive cross section for the CO^++H_2→ HCO^++H reaction, obtaining a related rate constant value ranging between 1.6 x10^{-9} and 3.0x10^{-9} cm^3 s^{-1} in the collision energy range of 0.01 – 3.0 eV, indicating a pronounced decline at elevated collision energies, higher than 7.0 eV [58]. An analogous situation has been recorded by Farrar and coworkers in their study of H_2^++CO proton transfer reaction producing HCO^+ in the 0.74 - 9.25 eV collision energy range [59]: at higher energies, the cross section drops rapidly whereas, at low energies, the HCO^+ products are highly excited, with 90% of the available energy in internal excitation.

A first consideration can be made regarding the production of a low energy CO_2-H_2 plasma. In such a case, it has to be noted that, by using CO^+ ions coming from the Coulomb explosion of CO_2^{2+} molecular dication, a projectile reactive species is available with a translational energy content of about 2.0-2.5 eV (see Fig.9). This means that in our plasma the CO^++H_2 reaction, also favored by a stronger long range trapping attraction, can occur with a

363 rate constant value higher than those of neutral-neutral reactions (having in most cases typical
364 rate constant values of about 10^{-10}-10^{-12} cm^3 s^{-1} [60]). In the case of the production of high
365 energy CO_2-H_2 plasmas, further considerations can be made, in order to take into account that
366 the CO^++H_2 measured cross section shows a strong decrease when the collision energy
367 becomes higher than 7 eV [58]. In this case, Knott *et al.* explain their results by invoking a
368 dissociation process of the HCO^+ product with a threshold beyond 7.0 eV. In fact, since CO^+
369 ($^2\Sigma$ simmetry) has a predissociating state close to 8.0 eV (vertical) [61] and the vertical
370 transition to the first excited state of H_2 ($^3\Sigma^+_u$) represents a step of about 9.0 eV, the CO^++H_2
371 collision should result in an excitation of CO^+ rather than of H_2. We fully agree with such
372 authors and it is important to note that the possible predissociation of CO^+ appears to be
373 energetically accessible at lower energies (about 5 eV) as demostrated by more recent
374 calculations by Okada and Iwata [62]. Furthermore, Nobes and Radom in 1981 [63] first
375 calculated the energy profile for the fast isomerization reaction between HCO^+ and COH^+
376 demonstrating a higher stability for HCO^+ and a triangular structure of the $[HCO]^+$
377 intermediate complex. This corroborates the absence of H_2^++CO and CO+H^++H possible
378 competitive products in the CO^++H_2 reaction for which Knott *et al.* [58] have recorded only
379 HCO^+ ions with any evidence of both H_2^+ and H^+ products. In their analysis such authors,
380 following ref. [61], did not consider the possibility of the HCO^+ with the rupture of the C---O
381 bond, because their relatively low investigated collision energy range. Moreover, such a
382 dissociation process is energetically allowed and can occur in high energy CO_2-H_2 plasmas,
383 where the formed HCO^+ ions are compatible with electron attachment dissociation processes
384 towards the production of CH+O neutral reactive species, as demonstrated since 1972 by
385 McGregor and Berry [64].

386 Finally, the efficient conversion of CO^+ and CO_2^+ ions into HCO^+ by collisions with
387 H_2 and H reactive partners (all these species can be formed in a CO_2-H_2 plasma), with the

388 $HOC^+ \leftrightarrow COH^+$ isomerization, has been experimentally observed by Gerlich and coworkers
389 [65, 66] and by Tosi *et al.* [67], corroborating the observation that in plasma environments
390 HCO^+ results a very stable species as it is confirmed by astronomical observations indicating
391 HCO^+ as one of the most important ions in dense molecular clouds [68,69].
392 In conclusion, it appears that the production of a CO_2-H_2 plasma by a microwave discharge
393 allowed us to generate: i) a large dissociation of carbon dioxide, according to reactions (12)
394 and (13) (see data of Table 1); and ii) CO_2^+, CO_2^{2+}, CO^+ and O^+ionic species (see reactions
395 (15)-(17) and Figures 8 and 9) able to react with atomic and molecular hydrogen in order to
396 produce HCO^+ ions. All such experimental evidences are compatible with the possible
397 formation of CH and CH+ species, being the first hydrogenation step on the carbon atom, for
398 a plasma-assisted CO_2 conversion into hydrocarbons as an alternative transformation route in
399 synthetic fuel processing.
400 Further experimental work is in progress in our laboratory in order to investigate such
401 possibility, and to optimize the experimental conditions in an attempt to perform the CO_2
402 hydrogenation reaction (5) via an alternative microscopic mechanism with respect to the use
403 of the solid catalyst.
404

405 **5. Conclusions**

406 The reported concerted efforts of University, ENEA and SMEs researchers in
407 investigating engineering and distributed computing have shown in this paper to what extent
408 the advances in basic research on plasmas are amenable to the assembling of an experimental
409 prototype applying the Sabatier reaction to a homogenous gas phase catalytic environment
410 and to the activation of a circular process turning waste CO_2 flue gases into methane. The
411 measurements performed have not only shown the viability of the proposed solution but have
412 also allowed the extension of computer simulations to a family of innovative mechanisms.

Furthermore, as a result of the investigation, useful indications have ben obtained on how to proceed to develop alternative solutions to the present Ni catalysed Progeo apparatus by resorting to a gas-phase-only process for the reduction of CO_2 to CH_4.In this work new results obtained by electrical discharges into CO_2-H_2 gas mixtures by using molecular beam technique at different pressure regimes has been presented. Such results together with VUV CO_2 photoionization data collected by synchrotron radiation are then of great help in identifying the microscopic mechanisms to be exploited. Finally, the production of a CO_2-H_2 plasma by a microwave discharge allowed us to generate a large dissociation of carbon dioxide, and to produce CO_2^+, CO_2^{2+}, CO^+ and O^+ ionic species able to react with atomic and molecular hydrogen in order to produce HCO^+ ions. All such experimental evidences are compatible with the possible formation of CH and CH+ species, representing the first hydrogenation step on the carbon atom, for a plasma-assisted CO_2 conversion into hydrocarbons. This is an alternative transformation route in synthetic fuel processing that we shall investigate further to the end of grounding Progeo on more robust methanation processes.

Acknowledgements

Financial contributions from the MIUR (Ministero dell'Istruzione, dell'Università e della Ricerca) through PRIN 2009 (Grant 2009W2W4YF_002) project is gratefully acknowledged. The authors also gratefully thank "Fondazione Cassa di Risparmio di Perugia" for partial supports (Project code: 2014.0255.021).

435 **References**

436 [1]Laganà A, Riganelli A.Reaction and molecular dynamics.Berlin, Heidelberg, New York:
437 Springer-Verlag; 2000. ISBN:3-540-41202-6

438 [2] Lombardi A, Faginas Lago N, Laganà A, Pirani F, Falcinelli S. A Bond-Bond Portable
439 Approach to Intermolecular Interactions: Simulations for N-methylacetamide and Carbon
440 Dioxide Dimers. O. Gervasi et al. (Eds.): ICCSA 2012, Part I, LNCS 2012; 7333: 387–
441 400.DOI: 10.1007/978-3-642-31125-3_30

442 [3] Falcinelli S, Rosi M, Candori P, Vecchiocattivi F, Bartocci A, Lombardi A, Faginas Lago
443 N, Pirani F. Modeling the Intermolecular Interactions and Characterization of the Dynamics
444 of Collisional Autoionization Processes. O. Gervasi et al. (Eds.): ICCSA 2013, Part I, LNCS
445 2013; 7971: 69–83.DOI: 10.1007/978-3-642-39637-3_6

446 [4] Cappelletti D, Bartocci A, Grandinetti F, Falcinelli S, Belpassi L, Tarantelli F, Pirani F.
447 Experimental Evidence of Chemical Components in the Bonding of Helium and Neon with
448 Neutral Molecules. Chem Eur J 2015; 21: 6234-40. DOI: 10.1002/chem.201406103

449 [5] Brunetti B, Candori P, Falcinelli S, Lescop B, Liuti G, Pirani F, Vecchiocattivi F. Energy
450 dependence of the Penning ionization electron spectrum of $Ne^*(^3P_{2,0})$+Kr. Eur Phys J D 2006;
451 38: 21-7. DOI: 10.1140/epjd/e2005-00312-5

452 [6] Alagia M, Bodo E, Decleva P, Falcinelli S, Ponzi A, Richter R, Stranges S. The soft X-ray
453 absorption spectrum of the allyl free radical. Phys Chem Chem Phys 2013; 15: 1310-8. DOI:
454 10.1039/c2cp43466k

455 [7] Falcinelli S, Rosi M, Pirani F, Stranges D, Vecchiocattivi F. Measurements of Ionization
456 Cross Sections by Molecular Beam Experiments: Information Content on the Imaginary Part
457 of the Optical Potential. J Phys Chem A 2016; 120: 5169-74. DOI: 10.1021/acs.jpca.6b00795

458 [8] Cappelletti D, Falcinelli S, Pirani F. The Intermolecular Interaction in D_2-CX_4 and O_2-CX_4
459 (X=F, Cl) Systems: Molecular Beam Scattering Experiments as a Sensitive Probe of the

460 Selectivity of Charge Transfer Component. J Chem Phys 2016; 145: 134305. DOI:
461 10.1063/1.4964092
462 [9] Personal Web site of Andrea Capriccioli, www.afs.enea.it/capricci/andrea.html [accessed
463 18.02.17]
464 [10] European Cooperation in Science and Technology, COST Actions, Chemistry and
465 Molecular Sciences and Technologies (CMST) - D37,
466 www.cost.eu/COST_Actions/cmst/D37[accessed 18.02.17]
467 [11] European Cooperation in Science and Technology, COST Actions, Chemistry and
468 Molecular Sciences and Technologies (CMST) – CM1404,
469 www.cost.eu/COST_Actions/cmst/CM1404[accessed 18.02.17]
470 [12] Laganà A, Riganelli A, Gervasi O. On the structuring of the computational chemistry
471 virtual organization COMPCHEM. Lecture Notes in Computer Science 2006; 3980: 665-74.
472 DOI: 10.1007/11751540_70
473 [13] EGI Web site, VT Towards a CMMST VRC, General project information,
474 https://wiki.egi.eu/wiki/VT_Towards_a_CMMST_VRC [accessed 18.02.17]

475 [14] Birbara PJ, Sribnik F. Development of an improved Sabatier reactor. Am Soc Mech Eng
476 1979; 7936: 1-10.

477 [15] ZACROS Kinetic Monte Carlo software package Web site,http://zacros.org/ [accessed
478 18.02.17]
479 [16] Müller-Krumbhaar H, Binder K. Dynamic properties of the Monte Carlo method in
480 statistical mechanics. J Stat Phys 1973; 8: 1-24. DOI:10.1007/BF01008440
481 [17] Bortz AB, Kalos MH, Lebowitz JL. A new algorithm for Monte Carlo simulation of ising
482 spin systems. J Comput Phys 1975: 17: 10-18. DOI:10.1016/0021-9991(75)90060-1

[18] Laganà A, Costantini A, Gervasi O, Faginas-Lago N, Manuali C, Rampino S. COMPCHEM: Progress Towards GEMS a Grid Empowered Molecular Simulator and Beyond. J Grid Computing 2010; 8: 571-86. DOI:10.1007/s10723-010-9164-x

[19] Martì C, Pacifici L, Laganà A. Networked computing for ab initio modeling the chemical storage of alternative energy: Third term report (March-May 2016). VIRT&L-COMM.9.2016.5 Errata corrige in the caption of Fig. 2 “ref. 14” should read “ref. 9”.

[20] Anslyn EV, Doughtery DA. Transition State Theory and Related Topics. In: Modern Physical Organic Chemistry, University Science Books; 2006, p. 365–73. ISBN:1-891389-31-9

[21] Ren J, Guo H, Yang J, Qin Z, Lin J, Li Z. Insights into the mechanisms of CO_2 methanation on Ni(111) surfaces by density functional theory. Applied Surface Science 2015; 351: 504–16. DOI: 10.1016/j.apsusc.2015.05.173

[22] Martì C, Pacifici L, Capriccioli A, Laganà A. Simulation of Methane Production from Carbon Dioxide on a Collaborative Research Infrastructure. O. Gervasi et al. (Eds.): ICCSA 2016, Part I, LNCS 2016; 9786: 319–33. DOI: 10.1007/978-3-319-42085-1_25

[23] Ziff RM, Gulari E, Barshad Y. Kinetic phase transitions in an irreversible surface-reaction model. Phys. Rev. Letter 1986; 2553-56. DOI: PhysRevLett.56.2553

[24] Brunetti B, Cappelletti D, Falcinelli S, Liuti G, Pirani F. Atomic and molecular beams from electrical discharges: their characterization and applications useful for plasma diagnostic and chemical modelling. In “ISPC 12 – International Symposium on Plasma Chemistry Proceedings”, Ed. by J.V. Heberlein, D.W. Ernie, J.T. Roberts (Minneapolis, Minnesota, USA); 1995: 1: 343-8. ISBN: 1-887976-01-9

[25] Brunetti BG, Falcinelli S, Giaquinto E, Sassara A, Prieto-Manzanares M, Vecchiocattivi F. Metastable Metastable-Idrogen-Atom Scattering by Crossed Beams: Total Cross Sections

for H^*(2s)-Ar, Xe, and CCl_4 at Thermal Energies. Phys Rev A 1995; 52: 855-8. DOI: 10.1103/PhysRevA.52.855

[26] Brunetti BG, Candori P, De Andres J, Falcinelli S, Stramaccia M, Vecchiocattivi F. Metastable Hydrogen Atom Scattering by Crossed Molecular Beams: Total Cross-Sections for H(2s)-Kr, O_2, and Cl_2 at Thermal Energies. Chem Phys Lett 1998; 290: 17-23. DOI: 10.1016/S0009-2614(98)00463-1

[27] Falcinelli S, Rosi M, Candori P, Vecchiocattivi F, Farrar JM, Pirani F, et al. Kinetic energy release in molecular di-cations fragmentation after VUV and EUV ionization and escape from planetary atmospheres. Plan Space Sci 2014; 99: 149–57. DOI: 10.1016/j.pss.2014.04.020

[28] Falcinelli S, Pirani F, Alagia M, Schio L, Richter R, Stranges S, et al. Molecular Dications in Planetary Atmospheric Escape. Atmosphere 2016; 7: 112. DOI: 10.3390/atmos7090112

[29] Falcinelli S, Pirani F, Alagia M, Schio L, Richter R, Stranges S, Vecchiocattivi F. The escape of O^+ ions from the atmosphere: An explanation of the observed ion density profiles on Mars. Chem Phys Lett 2016; 666: 1-6. DOI: 10.1016/j.cplett.2016.09.003

[30] Falcinelli S, Bartocci A, Cavalli S, Pirani F, Vecchiocattivi F. Stereo-dynamics in collisional autoionization of water, ammonia, and hydrogen sulfide with metastable rare gas atoms: competition between intermolecular halogen and hydrogen bonds. Chem Eur J 2016; 22: 764-71. DOI: 10.1002/chem.201503692

[31] Falcinelli S, Rosi M, Cavalli S, Pirani F, Vecchiocattivi F. Stereoselectivity in Autoionization Reactions of Hydrogenated Molecules by Metastable Noble Gas Atoms: The Role of Electronic Couplings. Chem Eur J 2016; 22: 12518-26. DOI: 10.1002/chem.201601811

[32] Alagia M, Callegari C, Candori P, Falcinelli S, Pirani F, Richter R, et al. Angular and energy distribution of fragment ions in dissociative double photoionization of acetylene molecules at 39 eV. J Chem Phys 2012; 136: 204302. DOI: 10.1063/1.4720350

[33] Falcinelli S, Alagia M, Farrar JM, Kalogerakis KS, Pirani F, Richter R, et al. Angular and energy distributions of fragment ions in dissociative double photoionization of acetylene molecules in the 31.9-50.0 eV photon energy range. J Chem Phys 2016; 145: 114308. DOI: 10.1063/1.4962915

[34] Brunetti B, Candori P, Cappelletti D, Falcinelli S, Pirani F, Stranges D, Vecchiocattivi F. Penning Ionization Electron Spectroscopy of water molecules by metastable neon atoms. Chem Phys Lett 2012; 539: 19-23. DOI: 10.1016/j.cplett.2012.05.020

[35] Falcinelli S, Pirani F, Vecchiocattivi F. The Possible role of Penning Ionization Processes in Planetary Atmospheres.Atmosphere 2015; 6: 299–317. DOI: 10.3390/atmos6030299

[36] Biondini F, Brunetti BG, Candori P, De Angelis F, Falcinelli S, Tarantelli F, et al. Penning ionization of N_2O molecules by $He^*(2^{3,1}S)$ and $Ne^*(^3P_{2,0})$ metastable atoms: A crossed beam study. J Chem Phys 2005; 122: 164307. DOI: 10.1063/1.1884604

[37] Cappelletti D, Candori P, Falcinelli S, Albertì M, Pirani F. A molecular beam scattering investigation of methanol-noble gas complexes: characterization of the isotropic potential and insights into the nature of the interaction. Chem Phys Lett 2012; 545: 14-20. DOI: 10.1016/j.cplett.2012.07.020

[38] Balucani N, Bartocci A, Brunetti B, Candori P, Falcinelli S, Pirani F, et al. Collisional autoionization dynamics of $Ne^*(^3P_{2,0})$-H_2O. Chem Phys Lett 2012; 546: 34-9. DOI: 10.1016/j.cplett.2012.07.051

[39] Dobrea S, Mihaila I, Popa G. Carbon dioxide dissociation in a 2.45 GHz microwave discharge. 31st ICPIG, Granada, Spain; 2013: 14.

[40] Dobrea S, Mihaila I, Tiron V, Popa G. Optical and mass spectrometry diagnosis of a CO_2 microwave plasma discharge. Romanian Reports in Physics 2014; 66: 1147-54.

[41] Welzel S, Brehmer F, Ponduri S, Creatore M, van de Sanden MCM, Engeln R. Plasma-assisted CO_2 conversion as alternative to conventional fuel processing. 30st ICPIG, Belfast, Northern Ireland, UK; 2011: D16.

[42] Blyth RR, Delaunay R, Zitnik M, Krempasky J, Slezak J, Prince KC, et al. The high resolution Gas Phase Photoemission beamline, Elettra. J Electron Spectrosc Relat Phenom 1999; 101–103: 959-64. DOI: 10.1016/S0368-2048(98)00381-8

[43] Alagia M, Candori P, Falcinelli S, Lavollée M, Pirani F, Richter R, et al. Double photoionization of N_2O molecules in the 28-40 eV energy range.Chem Phys Lett2006;432: 398-402. DOI: 10.1016/j.cplett.2006.10.100

[44] Alagia M, Candori P, Falcinelli S, Lavollèe M, Pirani F, Richter R, et al. Anisotropy of the angular distribution of fragment ions in dissociative double photoionization of N_2O molecules in the 30-50 eV energy range. J Chem Phys 2007; 126: 201101. DOI: 10.1063/1.2743616

[45] Alagia M, Candori P, Falcinelli S, Pirani F, Pedrosa Mundim MS, Richter R, et al. Dissociative double photoionization of benzene molecules in the 26–33 eV energy range. Phys Chem Chem Phys 2011; 13: 8245-50. DOI: 10.1039/c0cp02678f

[46] Lavollée M. A new detector for measuring three-dimensional momenta of charged particles in coincidence. Rev Sci Instrum 1990: 70: 2968-74. DOI: 10.1063/1.1149855

[47] Witasse O, Dutuit O, Lilensten J, Thissen R, Zabka J, Alcaraz C, et al. Prediction of a CO_2^{++} layer in the atmosphere of Mars. Geophys Res Lett 2002; 29: 1263. DOI: 10.1029/2002GL014781

[48] Lilensten J, Witasse O, Simon C, Soldi-Lose H, Dutuit O, Thissen R. Alcaraz C. Prediction of a N_2^{++} layer in the atmosphere of Titan. Geophys Res Lett 2005; 32: L03203.

581 DOI: 10.1029/2004GL021432

582 [49] Alagia M, Balucani N, Candori P, Falcinelli S, Pirani F, Richter R, et al. Production of
583 ions at high energy and its role in extraterrestrial environments. Rend Lincei Sci Fis Nat 2013;
584 24: 53-65. DOI: 10.1007/s12210-012-0215-z

585 [50] Thissen R, Witasse O, Dutuit O, Wedlund CS, Gronoff G, Lilensten J. Doubly-charged
586 ions in the planetary ionospheres: A review. Phys Chem Chem Phys 2011; 13: 18264-87.
587 DOI: 10.1039/C1CP21957J

588 [51] Lilensten J, Simon Wedlund C, Barthélémy M, Thissen R, Ehrenreich D, Gronoff G,
589 Witasse O. Dications and thermal ions in planetary atmospheric escape. Icarus 2013; 222:
590 169–87. DOI: 10.1039/C1CP21957J

591 [52] Sabzyan H, Keshavarz E, Noorisafa Z. Diatomic dications and anions. J Iran Chem Soc
592 2014; 11: 871-945. DOI: 10.1007/s13738-013-0359-5

593 [53] Franceschi P, Thissen R, Zabka J, Roithová J, Herman Z, Dutuit O. Internal energy
594 effects in the reactivity of CO_2^{2+} doubly charged molecular ions with CO_2 and CO. Int J Mass
595 Spectrom 2003;228: 507-16. DOI: 10.1016/S1387-3806(03)00157-X

596 [54] Slattery AE, Field TA, Ahmad M, Hall RI, Lambourne J, Penent F, et al. Spectroscopy
597 and metastability of CO_2^{2+} molecular ions. J Chem Phys 2005;122: 084317. DOI:
598 10.1063/1.1850895

599 [55] Alagia M, Candori P, Falcinelli S, Lavollèe M, Pirani F, Richter R, et al. Double
600 Photoionization of CO_2 molecules in the 34-50 eV Energy range.J Phys Chem A 2009;113:
601 14755. DOI:10.1021/jp9048988

602 [56] Alagia M, Candori P, Falcinelli S, Lavollèe M, Pirani F, Richter R, et al. Dissociative
603 double photoionization of CO_2 molecules in the 36–49 eV energy range: angular and energy
604 distribution of ion products. Phys Chem Chem Phys 2010; 12: 5389-95. DOI:
605 10.1039/b926960f

606 [57] Lundqvist M, Baltzer P, Edvardsson D, Karlsson L, Wannberg B. Novel time of flight
607 instrument for doppler free kinetic energy release spectroscopy. Phys Rev Lett 1995; 75:
608 1058-61. DOI: 10.1103/PhysRevLett.75.1058
609 [58] Knott WJ, Proch D, and Pompa KL. The hydrogen atom abstraction reaction
610 $CO^+ + H_2 \rightarrow HCO^+ + H$: Translational and internal energy dependence of the integral cross
611 section. J Chem Phys 1998; 108: 527-33. DOI: 10.1063/1.475416
612 [59] Bilotta RM, Preuninger FN, and Farrar JM. Crossed beam study of the reaction H_2^+
613 (CO,H) HCO^+ from 0.74 to 9.25 eV. J Chem Phys 1980; 72: 1583-92. DOI:
614 10.1063/1.439357
615 [60] Atkinson R, Baulch DL, Cox RA, Hampson RF Jr., Kerr JA, Troe J. Evaluated Kinetic
616 and Photochemical Data for Atmospheric Chemistry: Supplement VIII, Halogen Species.
617 IUPAC Subcommittee on Gas Kinetic Data Evaluation for Atmospheric Chemistry. J Phys
618 Chem Ref Data 2000; 29: 167-266. DOI: 10.1063/1.556058
619 [61] Krishnamurthy M, and Mathur D. Collisional excitation of CO by slow molecular
620 ions: wavefunction overlap effects. J Phys B: At Mol Opt Phys 1994; 27: 1177-86. DOI:
621 10.1088/0953-4075/27/6/017
622 [62] Okada K, and Iwata S. Accurate potential energy and transition dipole moment curves
623 for several electronicstates of CO^+. J Chem Phys 2000; 112: 1804. DOI: 10.1063/1.480743
624 [63] Nobes RH, and Radom L. HOC^+: An observable interstellar species? A comparison
625 with the isomeric and isoelectronic HCO^+, HCN AND HNC. Chem Phys 1981; 60: 1-10.
626 DOI: 10.1016/0301-0104(81)80102-4
627 [64] MacGregor M, and Berry RS. Formation of HCO^+ by the associative ionization of
628 CH+O. J Phys B: At Molec Phys 1973; 6: 181-96. DOI: 10.1088/0022-3700/6/1/020
629 [65] Smith MA, Schlemmer S, von Richthofhen J, and Gerlich D. $HOC^+ + H_2$ isomerization
630 rate at 25 K: Implications for the observed $[HCO^+]/[HOC^+]$ ratios in the interstellar

631 medium.Astrophys J 2002; 578:L87–L90. DOI: 10.1086/344404

632 [66] Borodi G, Luca A, and Gerlich D. Reactions of CO_2^+ with H, H_2 and deuterated
633 analogues. Int J Mass Spectrom 2009; 280:218–25. DOI: 10.1016/j.ijms.2008.09.004

634 [67] Tosi P, Iannotta S, Bassi D, Villinger H, Dobler W, Lindinger W. The reaction of
635 CO_2^+ with atomic hydrogen. J Chem Phys 1984; 80:1905-6. DOI: 10.1063/1.446951

636 [68] Watson WD. Ion-Molecule Reactions, Molecule Formation, and Hydrogen-Isotope
637 Exchange in Dense Interstellar Clouds. Astrophys J 1974; 188:35-42. DOI: 10.1086/152681

638 [69] Bruna PJ, Peyerimhoff D, and Buenker RJ. Ab initio investigation of the HCO^+ and
639 COH^+ molecule-ions: Structure and potential surfaces for dissociation in ground and excited
640 states. Chem Phys 1975; 10:323-34. DOI: 10.1016/0301-0104(75)87046-7

641

642 **Table 1** – The percentage of CO_2 dissociation in microwave discharge plasma source
643 produced in pure CO_2 and in a 1:1 CO_2/H_2 gaseous mixture for different values of applied
644 microwave power. The percentage values are calculated using the simple equation (2), and are
645 collected working at a constant pressure of 1600 Pa into the plasma source (see text). The data
646 are compared with those previously collected by Dobrea *et al.* in an analogous experiment
647 performed at a constant pressure of about 600 Pa [41,42].

648

Microwave discharge power (W)	% of CO_2 dissociation in pure CO_2 plasma		% of CO_2 dissociation in a 1:1 CO_2/H_2 plasma mixture	
	This work	ref. [14]	This work	refs. [39,40]
70	19±4	---	11±4	---
100	27±3	23	19±3	14
150	40±3	---	28±3	---
200	51±2	48	36±2	33

649

650
651

652

Figure captions

Fig. 1. 2500X micrography of the commercial catalyser KATALCO$_{JM}$ 11-4MR (by courtesy of University of Rome Tor Vergata, Rome, Italy).

Fig. 2. A picture of the twin columns of the ProGeo reactor.

Fig. 3. Cross section of the reactor twin columns and locations of the related thermocouples (red dots). On the right hand side the labels of the thermocouples.

Fig. 4. Average measured percentage of the methane produced in our experiments plotted as a function of the molar ratio and of the temperature with a pressure of 2 bar.

Fig. 5. Relative contributions of the different elementary channels to the production of methane evaluated from the minimum energy path of the PES (triangle) and from the ZACROS simulation (diamonds, squares, reverse triangles for the different temperatures connected by solid lines). The green triangle is the value suggested in ref.[24].

Fig. 6. The crossed molecular beam apparatus (mainly used in Penning ionization studies and adapted for plasmas generation containing carbon dioxide) in which the secondary beam was maintained off in order to detect the main chemical species coming out as an effusive molecular beam from the plasma microwave discharge source (see text).

Fig. 7. The electron-ion extraction and detection system used for the electron-ion-ion coincidence measurements to characterize the charged species produced in the CO_2 plasma by tunable synchrotron radiation. Left panel: a scheme of the set-up with a typical coincidence spectrum recorded by the double photoionization of CO_2 at a photon energy of 44 eV (see text). Right panel: a picture of such a device.

Fig. 8. Measured cross sections for the three main processes observed in the CO_2 plasma generation by using synchrotron radiation in the energy range of 34-50 eV and the electron-ion-ion coincidence technique (see text).

Fig.9. Kinetic energy distributions for CO^+ and O^+ fragment ions originating by Coulomb explosion of CO_2^{2+} dication produced in the CO_2 plasma by tunable synchrotron radiation.

FIG. 1

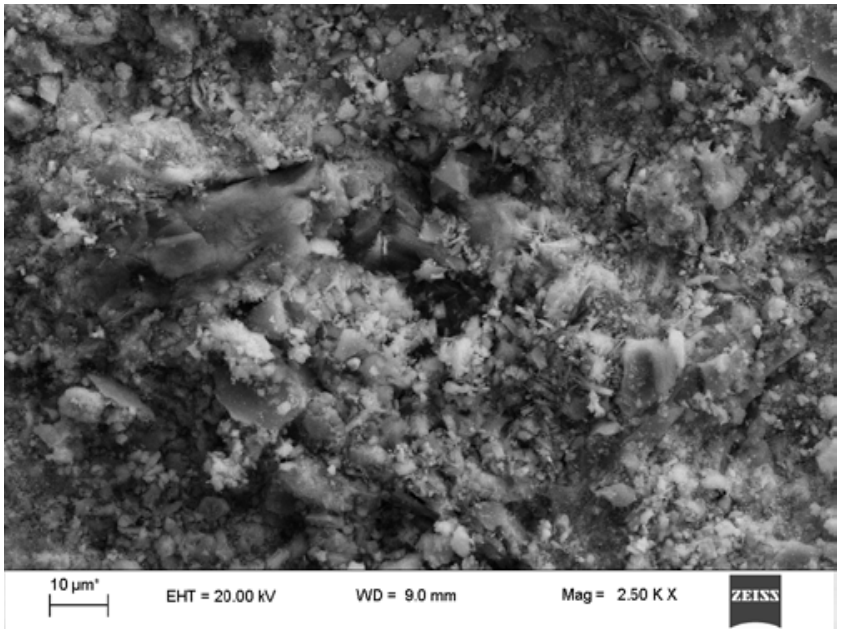

FIG. 2

FIG. 3

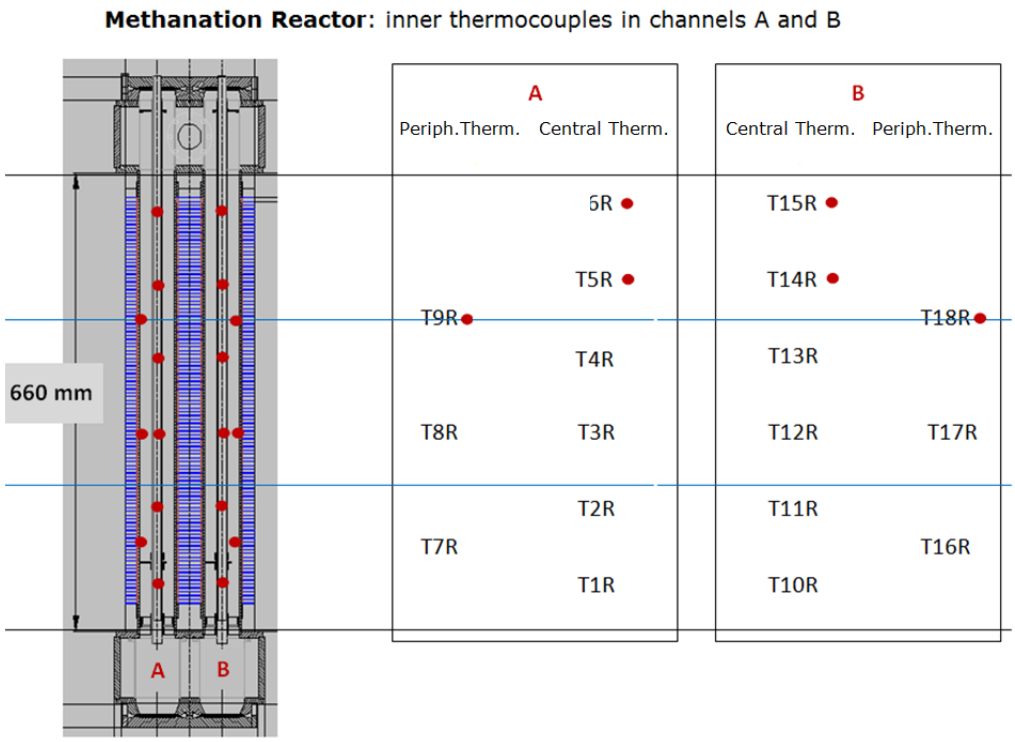

FIG. 4

T [°C] \ MR	4	4.5	5	5.5
240	47	56	65	68
245	49	58	66	70
250	51	60	68	72
255	52	62	69	74
260	54	63	70	75
265	56	65	71	77
270	57	67	73	78
275	58	68	74	79
280	60	69	75	81
285	61	70	77	82
290	62	71	78	82
295	63	72	79	83
300	64	73	80	84
305	64	73	81	84
310	65	74	82	84
315	65	74	82	84
320	66	74	83	84
325	66	74	83	84
330	66	74	83	84
335	66	73	83	83
340	66	73	82	82
345	65	72	81	82
350	65	71	80	80
355	64	70	79	79
360	64	69	77	78
365	63	67	75	76
370	62	66	72	74
375	60	64	69	72
380	59	62	66	70

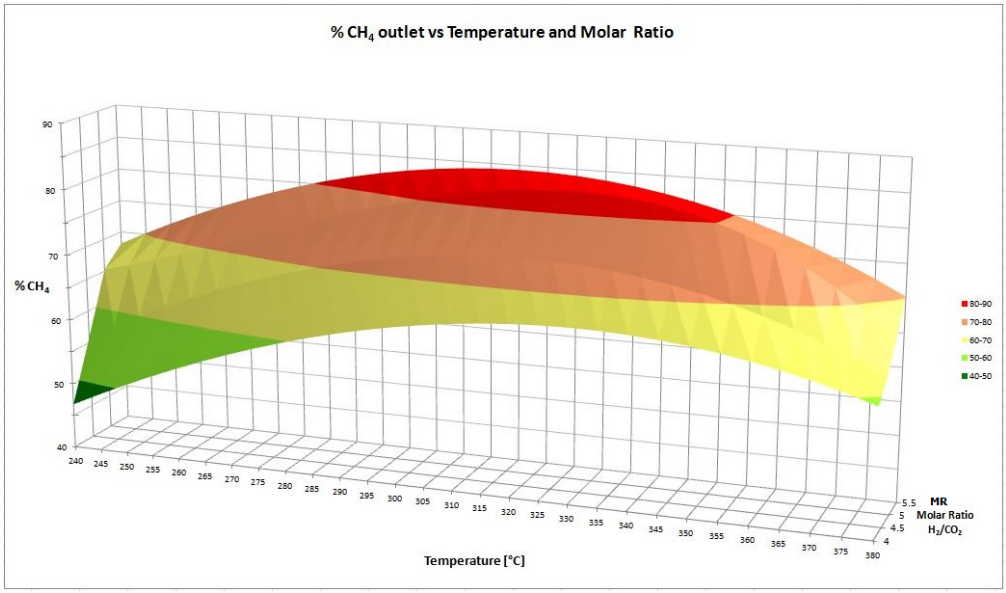

747 FIG. 5

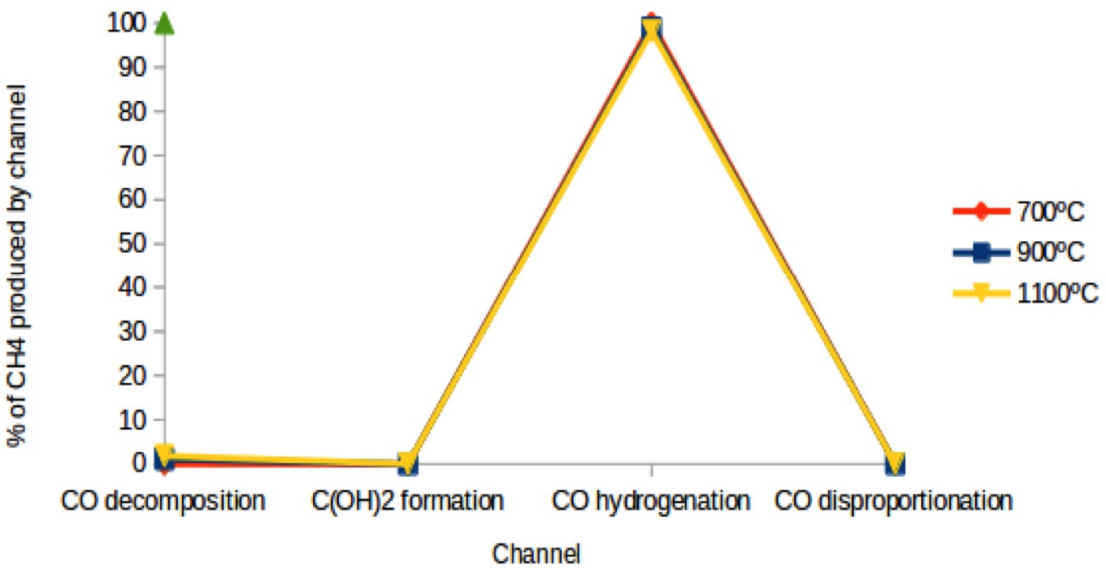

748

749

750 FIG. 6

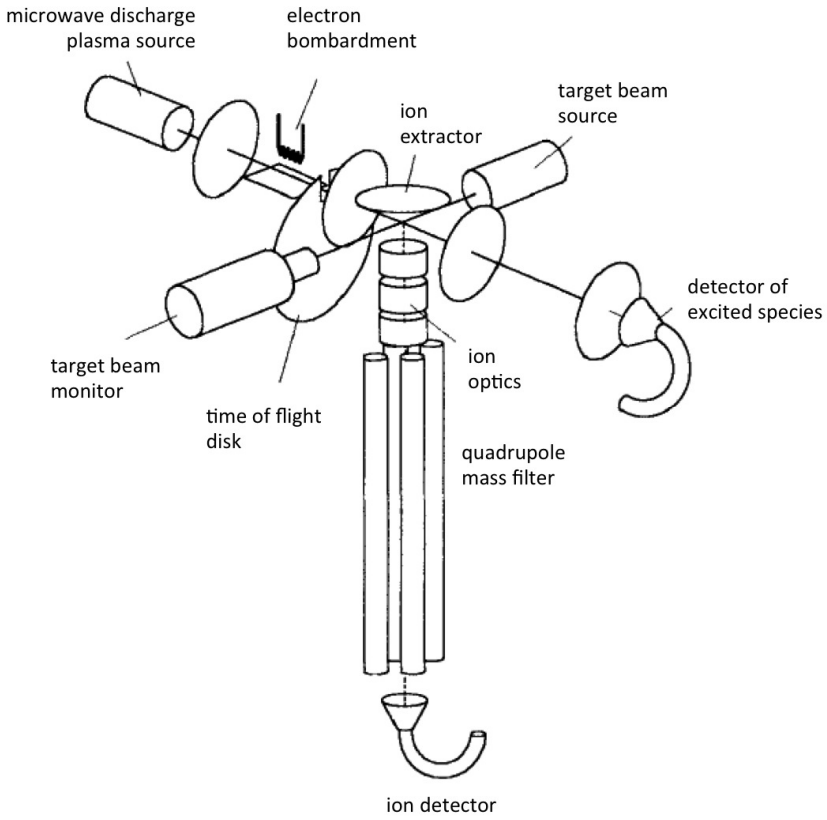

751

752 FIG. 7

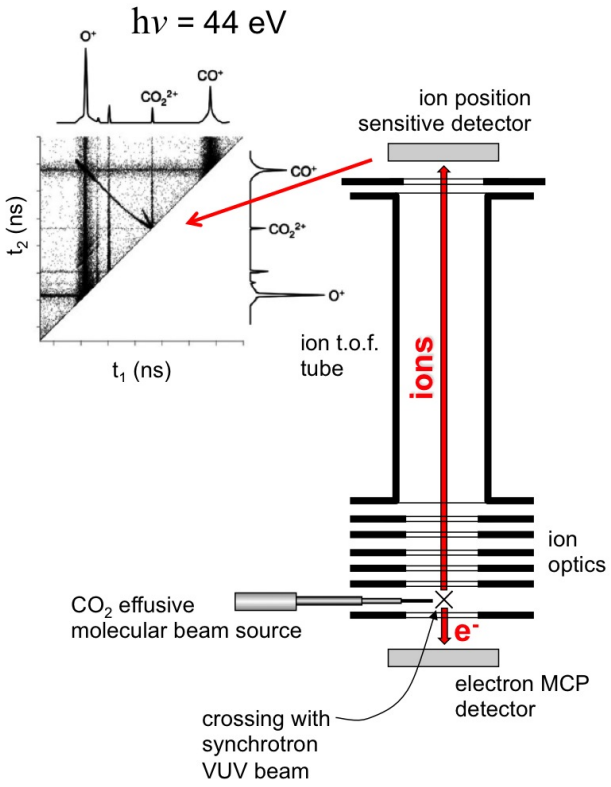
hν = 44 eV
O+
CO2 2+
CO+
t2 (ns)
t1 (ns)
CO+
CO2 2+
O+
ion position
sensitive detector
ion t.o.f.
tube
ions
ion
optics
CO2 effusive
molecular beam source
e-
electron MCP
detector
crossing with
synchrotron
VUV beam

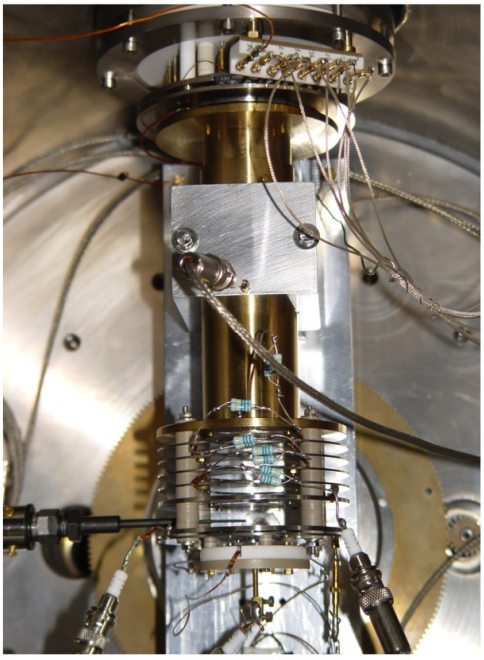

753

754

755 FIG. 8

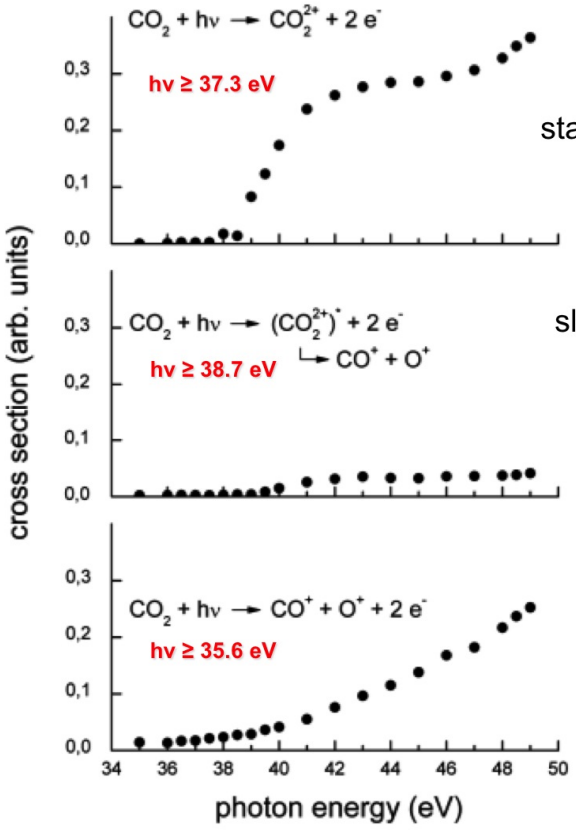

stable molecular dication formation
equation (15)

slow dissociation through long lived
dication metastable states
equation (16)

fast molecular fragmentation
equation (14)

756

757

758

759 FIG. 9

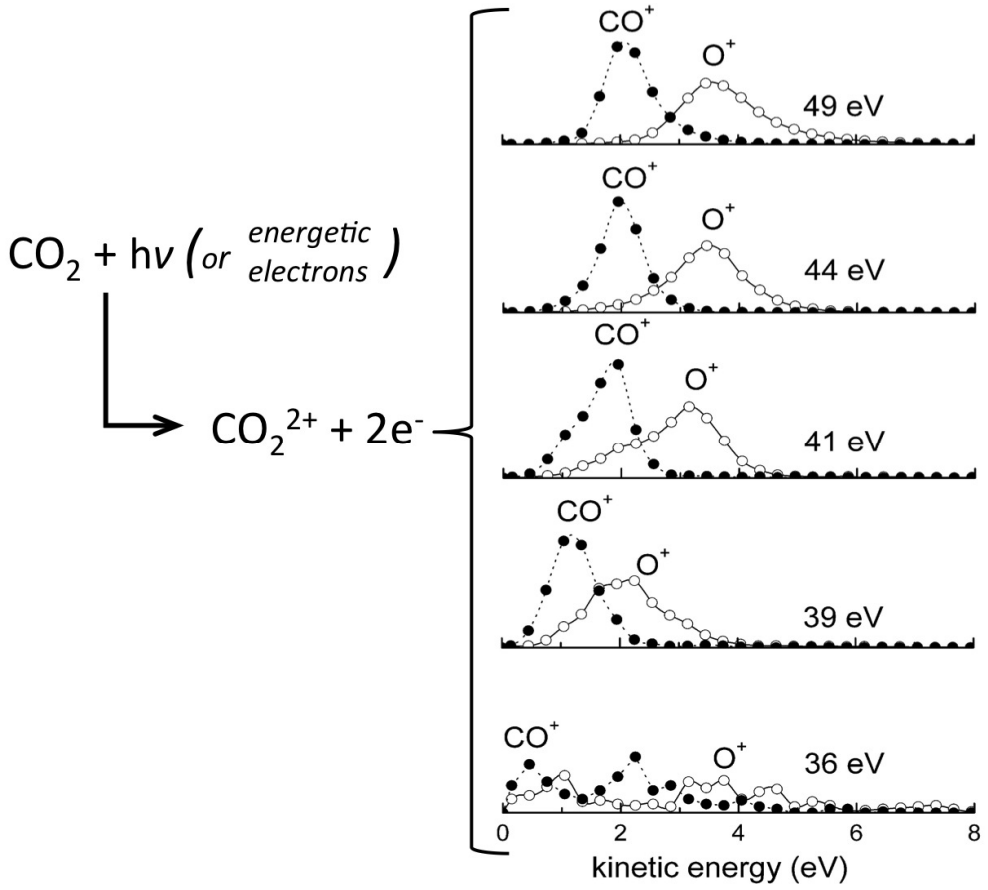

760

761